Fırat Üniversitesi Deneysel ve Hesaplamalı Mühendislik Dergisi

FUJECE

Elektriksel Akım Dalgasının and Frekansının Derin Beyin Stimülasyonu Üzerindeki Etkisinin Araştırılması

Enver SALKIM[1,2*]

[1]Elektronik ve Elektrik Mühendisliği Bölümü, College London (UCL) Üniversitesi, Londra, Birleşik Krallık.
[2]Elektronik ve Otomasyon Bölümü, Teknik Bilimler Meslek Yüksekokulu, Muş Alparslan Üniversitesi, Muş, Türkiye.
[1]e.salkim@ucl.ac.uk, [2]e.salkim@alparslan.edu.tr

Geliş Tarihi: 09.04.2024
Kabul Tarihi: 12.06.2024
Düzeltme Tarihi: 17.05.2024
doi: https://doi.org/10.62520/fujece.1467198
Araştırma Makalesi

Alıntı: E. Salkım, "Elektriksel akım dalgasının ve frekansının derin beyin stimülasyonu üzerindeki etkisinin araştırılması", Fırat Üni. Deny. ve Hes. Müh. Derg., vol. 4, no 1, pp. 59-71, Şubat 2025.

Öz

Biyo-hesaplamalı modellerin tıbbi cihazların tasarımı ve geliştirilmesi üzerinde önemli bir etkisi vardır. Bu yaklaşım, deneysel test kullanılarak tasarlanması mümkün olmayan çeşitli tıbbi cihaz parametre ayarlarının araştırılmasına olanak tanır. Bu nöromodülatör sistemler için en uygun parametrelerin kullanılması hasta güvenliği açısından çok önemlidir. Hesaplamalı modelleme, derin beyin stimülasyonunda (DBS) hedefleme ve stimülasyon parametrelerini iyileştirme mücadelesinde temel bir araçtır. Spesifik olarak, simülasyon dalga biçimi şekli, darbe genişliği ve amplitüdünün yanı sıra pasif faktörler de dahil olmak üzere birçok parametredeki farklılıklar nedeniyle DBS'yi birleştiren Parkinson hastalığı için optimal bir nöromodülatörün tasarlanması zor olabilir. Bu çalışma, bu tür gelişmiş biyo-hesaplamalı modelleme sistemlerini kullanarak farklı darbe genişliklerine dayalı farklı dalga formlarının kullanılmasının etkisini araştırmaktadır. Bir insan kafasının hacim iletkeni, temel doku katmanları da dahil olmak üzere ortalama insan kafası kalınlığına dayanılarak oluşturulmuştur. Daha sonra, farklı frekans aralıklarını kullanarak sonuçları analiz etmek için DBS elektrot dizisi tasarlandı ve hesaplamalı modelle birleştirildi. Ayrıca hesaplamalı model tasarımcıları için hesaplamalı model geliştirmenin temelleri vurgulandı. Daha sonra sonuçlar, zamana dayalı simülasyon kullanılarak elektrik ve akım yoğunluğu dağılımlarına göre hesaplandı. Simülasyon frekansının ve simülasyon dalga biçimi şeklinin sonuç üzerinde önemli bir etkiye sahip olduğu gösterilmiştir. Sonuçlar, ilgilenilen bölgedeki elektrik potansiyeli, akım yoğunluğu ve elektrik alan dağılımları üzerinde önemli bir etkiye sahip olması nedeniyle kapasitif etkinin daha yüksek frekans seviyelerinde göz ardı edilemeyeceğini göstermiştir.

Anahtar kelimeler: Biyo-hesaplamalı modelleme, Kapasitif etki, Derin beyin stimülasyonu, Simülasyon frekansı, Stimülasyon dalga formu

*Yazışılan yazar

İntihal Kontrol: Evet – Turnitin
Şikayet: fujece@firat.edu.tr

Firat University Journal of Experimental and Computational Engineering

Investigating Impact of Current Pulse Waveform and Simulation Frequency on Deep Brain Stimulation

Enver SALKIM[1,2*]

[1]Department of Electronic and Electrical Engineering, University College London (UCL), London, United Kingdom.
[2]Department of Electronic and Automation, Vocational School of Technical Sciences, Muş Alparslan University, Muş, Türkiye.
[1]e.salkim@ucl.ac.uk, [2]e.salkim@alparslan.edu.tr

Received: 09.04.2024
Accepted: 12.06.2024
Revision: 17.05.2024
doi: https://doi.org/10.62520/fujece.1467198
Research Article

Citation: E. Salkim, "Investigating impact of current pulse waveform and simulation frequency on deep brain stimulation", Firat Univ. Jour. of Exper. and Comp. Eng., vol. 4, no 1, pp. 59-71, February 2025.

Abstract

Bio-computational models have a significant impact on the design and development of medical devices. This approach allows investigation of various medical device parameter settings which would be infeasible to design by using the experimental test. Using the optimal parameters for these neuromodulator systems is crucial for the patient safety. Computational modelling is a fundamental tool in the challenge to improve targeting and stimulation parameters in deep brain stimulation (DBS). Specifically, it may be difficult to design an optimal neuromodulator for Parkinson's disease fusing DBS due to variations in many parameters including simulation waveform shape, pulse width, and amplitude as well as passive factors. This study investigates the impact of using different waveforms based on different pulse widths using such advanced bio-computational modelling systems. The volume conductor of a human head was generated based on average human head thickness including fundamental tissue layers. Then, the DBS electrode array was designed and merged with the computational model to analyse the results using different frequency ranges. Also, the fundamentals of the computational model developments were highlighted for the computational model designers. Then, the results were calculated based on electrical and current density distributions using time-based simulation. It was shown that the simulation frequency and simulation waveform shape have a significant impact on the outcome. The results suggested that the capacitive effect cannot be ignored at the higher frequency levels due to having a significant impact on the electrical potential, current density, and electric field distributions in the region of interest.

Keywords: Bio-computational modelling, Capacitive effect, Deep brain stimulation, Simulation frequency, Stimulation waveform

*Corresponding author

1. Introduction

It has been shown that it may not be possible to investigate the impact of the neuromodulator parameters on the target tissue layer using different electrode features based on experimental test or it is difficult to design an optimal medical device for individuals using clinical methods due to associated risks [1-3]. Computational modelling has been proven to be an effective tool for designing and analysing neuromodulator devices to treat health-related disorders and diseases. The general workflow for computational modelling of a neural stimulation device includes finite element (FE) models (FEM) involving, a volume conductor model representing various, anatomical structures and the electrodes by their respective conductivities and appropriate boundary conditions [4], as shown in Fig. 1 and 2.

It is possible to calculate the electrical potential distributions within the volume conductor of the computational models using available commercial FEM software packages (e.g., COMSOL Multiphysics, ANSYS). FEM has matured as a numerical. COMSOL Multiphysics (COMSOL, Ltd, Cambridge, UK) includes many matured numerical toolsets for solving bioelectric field problems with complex geometric features and anisotropic tissue properties [5-7]. However, it is not always clear how to generate the current source and implement the required boundary conditions accordingly. It has been shown that many studies were conducted based on the quasi-static approximation by neglecting capacitive and magnetic various applications. For example, the capacitive and magnetic affects were ignored when the electrode insertion guidance was analysed using FEM modelling approach [9, 10]. Also, the required stimulus current thresholds nerve fibers activation for various neuromodulator systems was calculated based on quasi-static approximation by ignoring capacitive affect using advanced bio-computational modelling [5, 8, 11-14]. There is not much information on designing current sources based on transient simulation using different simulation waveforms (e.g., sinusoidal, rectangular) simulation modes (biphasic, monophasic) as shown in Fig. 3. Designing and simulation of such parameters are crucial during the modelling as the results are used for many neural prostheses and therapies (include upper and lower limb prostheses for spinal cord injury and stroke and deep brain stimulation (DBS)) during the clinical tests. Then, the medical devices are designed and developed depending on the trial outcome [15].

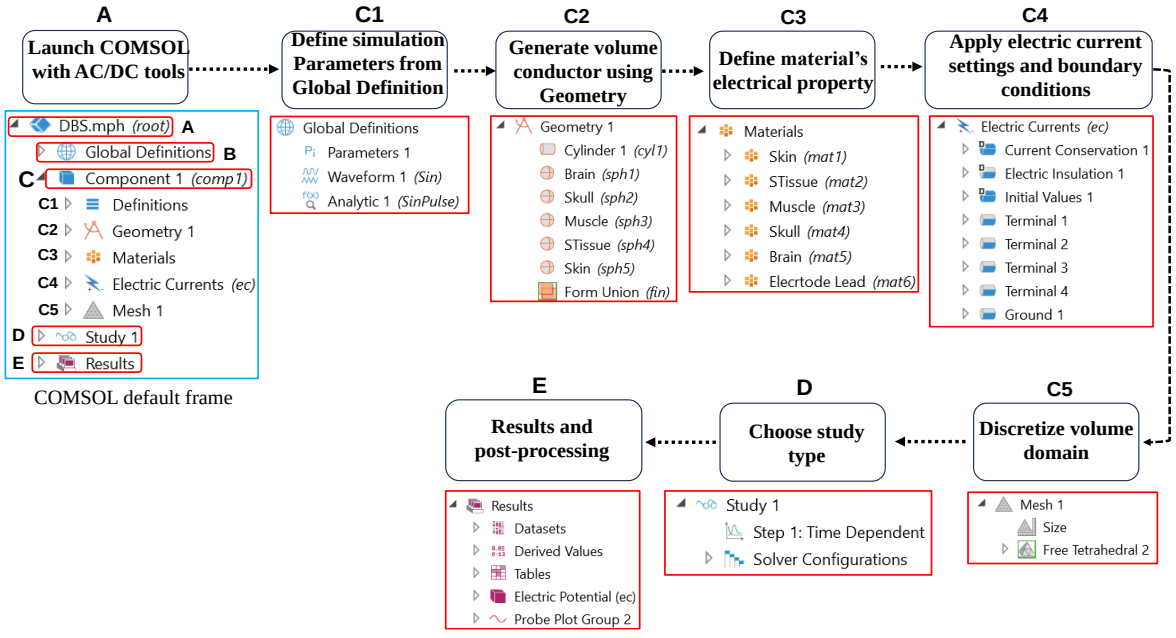

Figure 1. General workflow of COMSOL for AC/DC module. The default steps for AC/DC are shown. The steps for generating a computational model are numbered (from **A** to **E**)

The DBS is a neurosurgical procedure where an electrical stimulator is implanted in a specific brain region to treat multiple neuropsychiatric disorders, including Parkinson's disease. The DBS is a surgical procedure involving implantation of electrodes into deep the brain as shown in Fig. 2(a). The electrodes are placed to

the ROI using stereotactic or computer-assisted guidance techniques. The DBS has several advantages compared to the other surgical methods. Namely, the DBS is reversible, less interference with future intervention and adjustable to optimize benefit and reduce side effect. The main disadvantages of the DBS

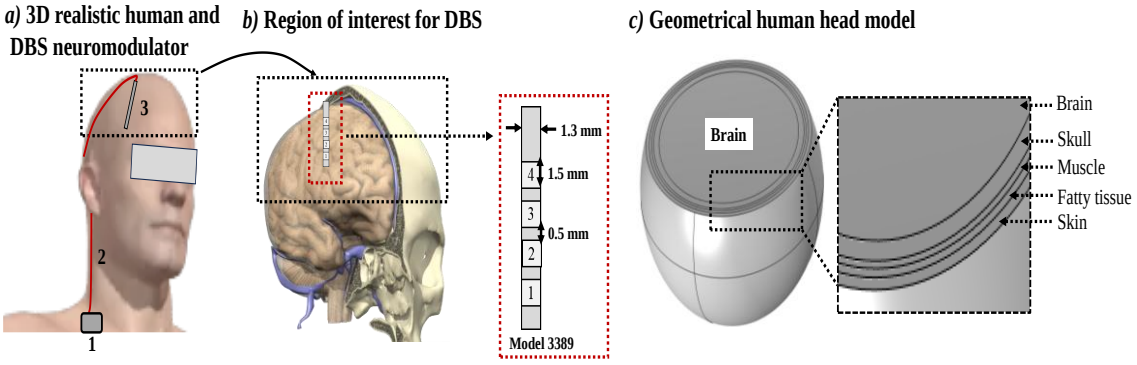

Figure 2. (***a***) Shows a simplified representation of the DBS system and its implementation inside the patient's head. (***b***) Shows the region of interest for the DBS. The electrode contacts are equally spaced, and the pitch of the electrode is set to 2 mm. (***c***) Shows the geometrical human head model that is generated based on the fundamental tissue layers

maybe it is more expensive, more time consuming, and it has complications related to device and the battery should be replaced periodically [16].

It has been shown that there are many parameters that affect the performance of the DBS neuromodulator including waveform shape, frequency, pulse width and amplitude as well as passive factors [17] The dielectric properties of the tissue are frequency dependence and may have a significant impact on the outcome. In particular, the electric field distribution is strongly influenced by the dielectric properties of the tissue layers, which have a heterogeneous, locally anisotropic, and dispersive nature. Also, the electrical field may show different results using a wide range of frequencies [18, 19]. Furthermore, the capacitive properties of grey and white matter cannot be disregarded for current-controlled stimulations [20]. Therefore, it is necessary to investigate the impact of such parameters. It is not feasible to investigate the impact of these various DBS neuromodulator parameters using experimental tests. Computational models of DBS generally rely on FEM to solve for the electrical potential distribution in the brain from the DBS pulses which otherwise impossible to do with experimental tests. The model used to solve for the DBS electrical potential distribution s called a volume conductor (VC) model [20]. The electrical potential distributions within the VC for DBS were extracted using isotropic dielectric parameters of each tissue layer [15]. The procedures of defining the DBS electrode contacts, the simulation settings and boundary conditions that represented in the finite element model can also affect the outcome as detailed in method section.

This paper investigates the impact of the simulation pulse waveform shape as well as the effect of dielectric properties of the anatomical layers based on different frequency on the current density and electrical potential distribution on the region of interest (ROI) (e.g. brain). Thus, current source based on different waveforms were designed in COMSOL Multiphysics using different electrode arrangements for DBS. Then, the time-based electric potential and current density distributions were calculated using conventional DBS electrode settings as shown in Fig. 2(b). The VC of the human head was developed using smooth geometrical shapes to analyse the impact of the current source waveforms based on the electrical potential distributions [3, 4]. The human head volume conductor was developed based on the fundamental tissue layers based concentric geometric shapes (e.g., sphere) as shown in as shown in Fig. 2(c). To mimic the realistic human head model, the layers were developed based on their average thickness [3], [4]. The main contributions of this study are:

- The human head model was developed, and the conventional DBS electrode model merged to analyse the impact of the different current pulse waveforms and simulation frequency levels on the outcome.
- The electrical potential and current density distributions were examined at the RIO by considering the safety criteria.

- By analysing the impact of the representations of the current sources for the electrical potential distribution using neuromodulator settings of DBS, the procedures of the more accurate and efficient simulation detailed, and useful recommendations were provided for the bio-computational model's designers.
-

The paper is organized as follows. The method section presents the development of the current source and boundary condition models; the results give the electrical potential distributions of chosen current source and the discussion and conclusion are given, respectively.

2. Methods

For all the subsequent simulations and operations, a computer with an Intel i7-8550U CPU @ 1.80GHz with 16GB RAM was used.

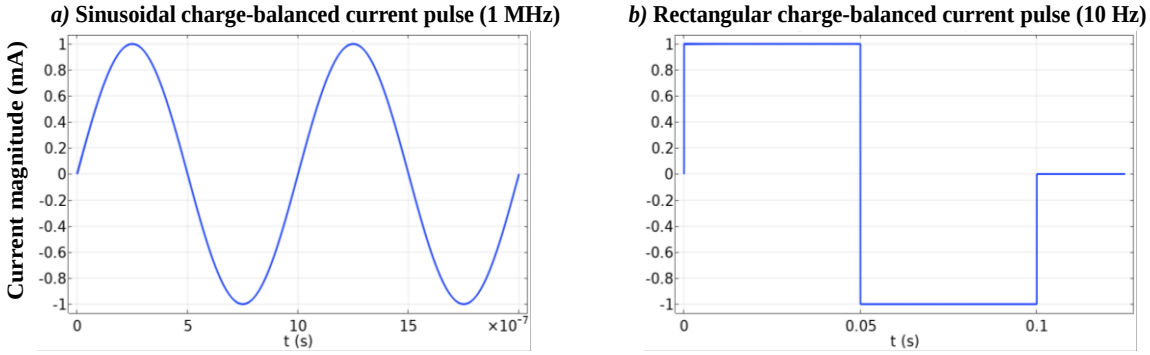

Figure 3. (***a***) Shows 1 MHz sinusoidal charge – balanced current pulse. (**b**) shows 10 Hz rectangular charge – balanced current pulse

2.1. Multi-layered model development

The computational model was generated using COMSOL Multiphysics based on the AC/DC module. The AC/DC module provides a unique environment for the simulation of electrical potential simulation in 2D and 3D. This module is a powerful tool for detailed analysis of the components of biomedical neuromodulators for various disorders.

The human head was generated using smooth geometrical shapes to investigate the impact of the simulation current source on the electrical potential distributions of DBS. The head model consisted of five concentric spheres to represent skin, fatty tissue, muscle, skull, and brain as detailed in Fig 2(c). Each layer was developed using its standard thickness (skin: 2.8 mm, fat: 2 mm, muscle: 1.7 mm, skull: 5.5 mm) to represent average individuals. Since the region of interest is the brain, and the electrical parameters of the grey and white matters are identical; the white and grey matters were combined and modelled as the brain. The brain layer was designed based on the average human brain diameter.

2.2. Electrode design

The DBS electrodes were designed based on commercially available neurostimulator for DBS therapy settings (Medtronic 3389) using smooth geometric shapes in COMSOL and the electrode model was inserted into the head model. The diameter of each electrode was set to 1.3 mm. The pitch of electrodes was chosen as 2 mm, as shown in Fig. 2(b). Each DBS lead included four contacts (4, 3, 2, 1) each contact has a length of 1.5 mm. The electrode was positioned in the ROI.
In the practical DBS, the electrical signal with a specific frequency was delivered to the target brain region via the neurostimulator, which is a pacemaker-like device installed subcutaneously near the clavicle of the

patient. However, the generated signal was directly applied to the electrode contacts as detailed in the following section.

2.3. Simulation source design

Since the simulation pulse of the DBS may affect the outcome, there is a need to investigate the impact of different pulse waveform shapes on the electrical potential and current density on the RIO. In general, the charge balanced pulse is used for the safety criteria [15] COMSOL Multiphysics allows researchers to design various current waveforms based on different pulse widths. Thus, the rectangular and sinusoidal balanced current pulses were generated based on 10 Hz and 1 MHz, respectively as shown in Fig. 3. After generating the current pulse, each pulse was named and applied to the electric contact of DBS electrode arrangements in the Electric current section. The current pulse for each contact was defined as in (1). It was noted that the current was given by Ampere (A) by default. Thus, if the lower amplitude is applied, the current should be converted to A. Since 1 mA current pulse was applied to the contacts, this value was used in (1).

$$I_0 = (0.001) * W(t)(A) \quad (1)$$

where I_0 is time-based the electrode contact current based on sinusoidal waveform. *W(t)* shows type of waveform source. Since the charge-balanced sinozoidal and rectangular current pulses were used in this study, $W(t) = Sin(\omega t)$ was used for the sinozidal current pulse and $W(t) = Rec(\omega t)$ was applied to the electrode contacts for the rectangular current pulse, ω shows angular frequency.

Table 1. Dielectric properties of huma head anatomical layers are based on different frequency levels.

Anatomical layers	Conductivity (σ) (10 Hz)	Relative permittivity (ε_r) (10 Hz)	Conductivity (σ) (1 MHz)	Relative permittivity (ε_r) (1 MHz)
Skin	2.00e-4	1.14e+3	1.32e-2	9.91e+2
Fatty tissue	3.77e-2	5.03e+6	4.41e-2	5.08e+1
Muscle	2.02e-1	2.57e+7	5.03e-1	1.84e+3
Skull	2.00e-2	5.52e+4	2.44e-2	1.45e+2
Brain	4.75e-2	4.07e+7	1.85e-1	1.14e+3

2.4. Electric properties of tissue and boundary conditions

The dielectric properties of the human head tissue layers were attained based on Table 1 for each simulation waveform. Since each tissue layer has different dielectric properties, each simulation was separately run by attaining associated features. The current simulation was designed based on a charge-balanced pulse for both waveforms to mimic the practical conditions. Thus, 1 mA current was applied to the anode contact and -1 mA was applied to the cathode contact for each simulation. Each electrode was defined as a contact boundary. Each electrode contact was defined as *Terminal* in COMSOL (*Terminal 1, Terminal 2, Terminal 3, Terminal 4).* The lead shaft was designed as an insulator with a conductivity of 10e-16 S/m, and the contacts were modelled as platinum/iridium with a conductivity of 5.3e6 S/m. The boundary components were built and consequently subtracted from the DBS lead model which resulted in external boundaries that were defined using boundary conditions. The Dirichlet boundary condition ($V = 0$) was applied at the near end of the electrode lead.

2.5. Finite element simulation

The accuracy of the simulation that can be obtained from any FEM is related to the finite element mesh settings during domain discretization. The finite element mesh is used to subdivide the defined domains into

smaller domains called elements to solve electrical potential distributions using underlying differential equations.

The VC of the human head and DBS electrode was discretized using the free tetrahedral element method as shown in Fig. 4(a). Since the electrode domain is relatively smaller in size, it was more finely meshed by modifying the maximum and minimum element size as shown in Fig. 4(b). The remaining domains were relatively coarsely meshed to reduce the computation time. These settings were applied until no significant difference was observed in the electrical potential variations based on given settings. This resulted in about 0.4 million tetrahedral elements and about 0.5 million degrees of freedom.
The transient time response of the given stimulation current pulses was studied based on the time-dependent electrical current approximation of Maxwell's equations using (2).

$$\nabla \cdot \left(\sigma \nabla V - \varepsilon_0 \varepsilon_r \nabla \frac{\partial V}{\partial t}\right) \tag{2}$$

where σ is the conductivity of each of the tissues, V is the electrical potential in the representative geometry, $\varepsilon_0 \varepsilon_r$ is the tissue permittivity.

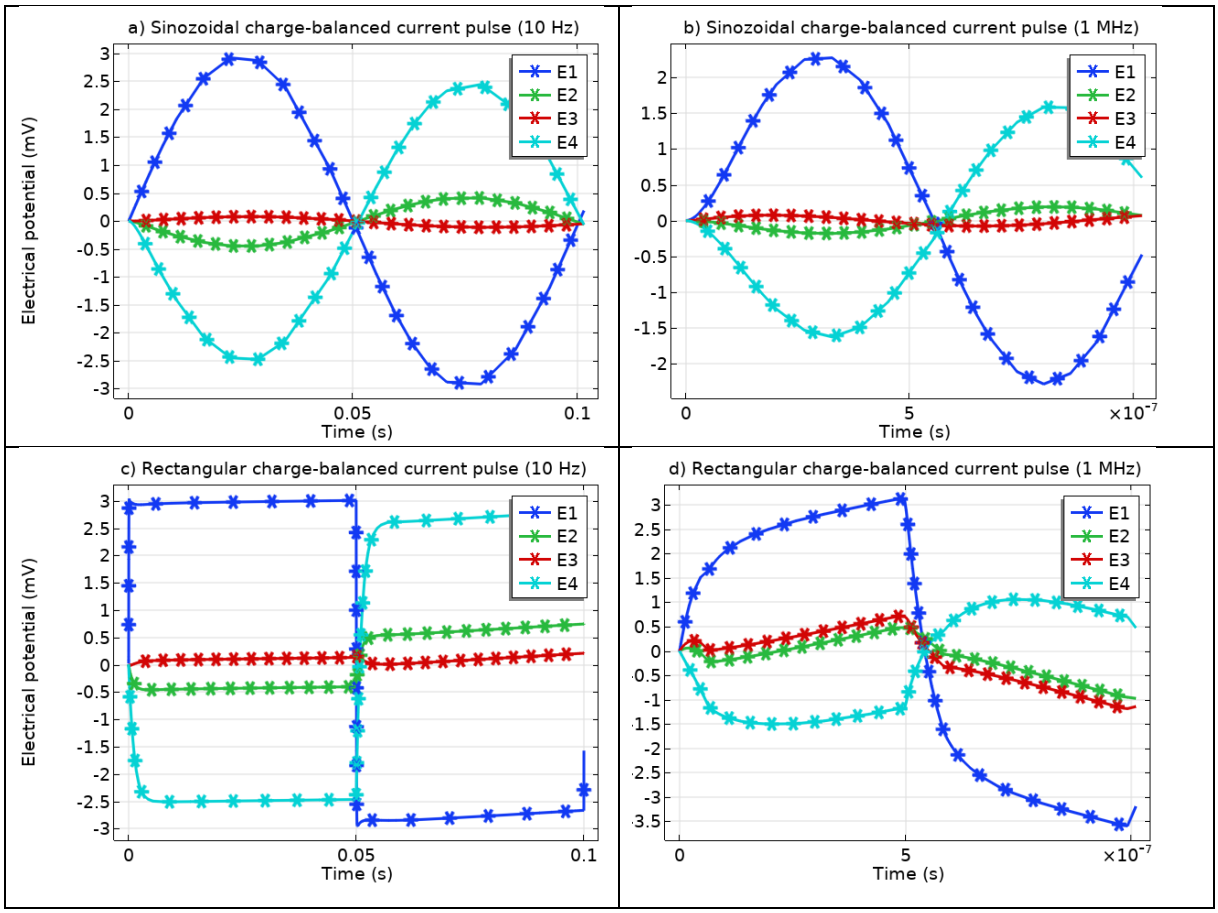

Figure 4. (***a***) Shows the electrical potential variation for 10 Hz using sinusoidal waveform. (***b***) shows the electrical potential variation for 1 MHz using sinusoidal waveform. (***c***) shows the electrical potential variation for 10 Hz using rectangular waveform. (***d***) shows the electrical potential variation for 1 MHz using rectangular waveform

The dielectric properties of each layer were attained using based on available data [3]. The electrode-tissue interface contact impedance was assumed to be zero and appropriate continuity conditions were implemented at the boundary of the different domains to have a unique solution. The current density distributions for 10

Hz and 1 MHz were compared using the same settings (e.g., the same contour number) for fair comparison. The results were recorded for each simulation as shown in Fig. 4(c).

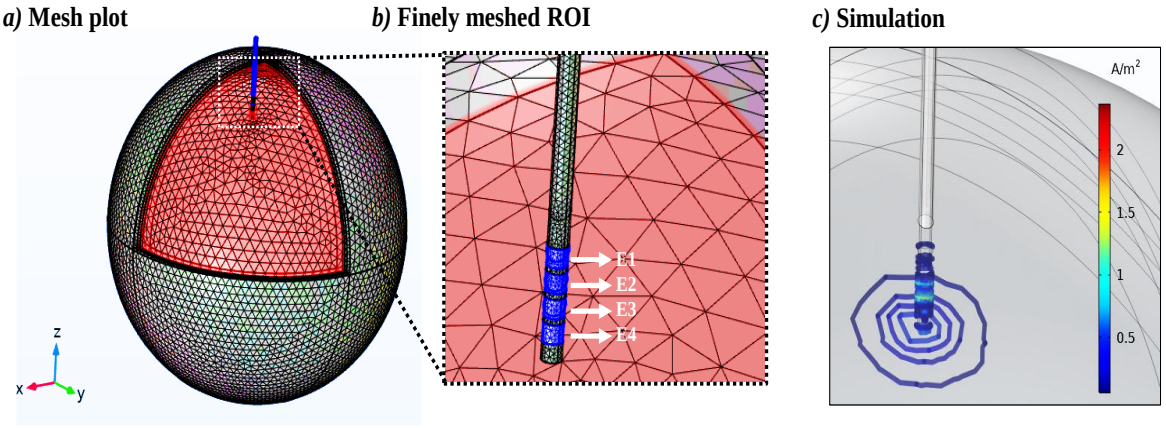

Figure 5. a) Shows volume conductor mesh plot. (b) Shows the region of interest (RIO) is relatively finely meshed. The electrode contacts are highlighted in blue and labelled in order (e.g. E1 to E4). (c) The results are recorded for each simulation pulse and frequency level

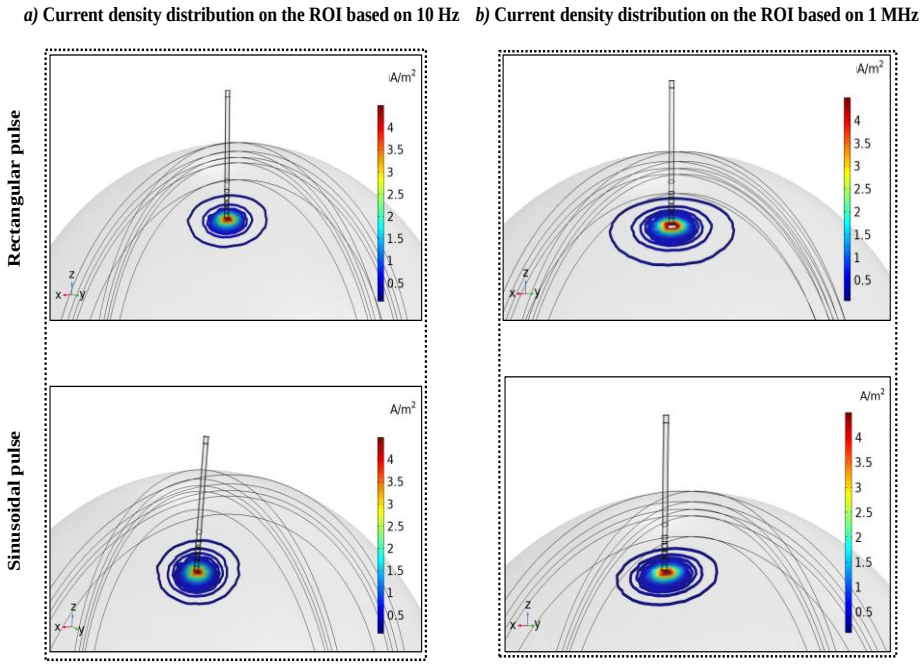

Figure 6. (***a***) Shows the current density variation for rectangular and sinusoidal waveforms based on 10 Hz. (***b***) Shows the current density variation for rectangular and sinusoidal waveforms based on 1 MHz

3. Results

3.1. Electrical potential

The electrical potential variation on the RIO for different simulation waveforms based on different simulation frequencies is shown in Fig. 5. The electrical potential variation was recorded for each frequency based on sinusoidal and rectangular simulation waveforms. The electrical potential variation based on sinusoidal

waveform is shown in Fig. 5(a) and (b). The electrical potential variation based on rectangular waveform is shown in Fig. 5(c) and (d). Each waveform is evaluated based on used frequencies as follows.

It is clearly shown that there is distortion in the stimulus current waveforms for both frequency ranges. The induced electrical potential range is about 6 mV for the 10 Hz frequency range. This is about 4 mV for the 1 MHz. The highest electrical potential variation is recorded for *Terminal 1* for both frequencies. Also, the lowest electrical potential induced on *Terminal 3* for both frequencies range.

Interestingly, the induced positive electrical potential range is higher for 1 MHz compared to 10 Hz using a rectangular stimulation waveform. However, the electrical potential range is the same for both simulation frequencies. The electrical potential value varies from -3 mV to 3 mV for 10 Hz. This varies from -0.5 mV to 5.5 mV for the 1 MHz. The recorded lowest electrical potential is observed on Terminal 3 for 10 Hz. The same trend is not observed for the 1 MHz.

It is also shown that the distortion in the rectangular electrical potential waveform is significantly distorted for 1 MHz, compared to the results for 10 Hz as shown in Fig. 5(d).

3.2. Current density

The current density variation on the RIO based on different frequency ranges using different simulation waveforms is shown in Fig. 6. The results for the 10 Hz and 1 MHz are shown in Fig. 6(a) and (b), respectively. The current density distributions are visualized with contours. The number of contours is the same for both simulation pulses and different frequency levels. The VC is unified based on grey colour and the current density variation is ranged with colormap in COMSOL to visualise current density over the RIO in more detail.

It is shown that the induced current density variation range was about the same for all waveforms and frequencies. It is clearly shown that the current density has a wide-spread range when 1 MHz current pulse is used, compared to 10 Hz. The current density has the same variation based on different current pulse waveforms for 10 Hz. It is noted that the results for the rectangular current pulse based on 1 MHz spread more on the RIO, compared to the sinusoidal current pulse based the 1 MHz.

3.3. Electrical Field

The electrical field distribution over the RIO based on different frequency ranges using different simulation waveforms is shown in Fig. 7. The electrical field is calculated based on *streamlines* in COMSOL to visualize variation on the surface of the RIO. The results for the 10 Hz and 1 MHz are shown in Fig. 7(a) and (b), respectively.

The higher value of the electric field is recorded for the rectangular waveform pulse for both frequency levels, compared to the sinusoidal current pulse. The electric field range is 0 to 60 V/m for the rectangular current pulse using 10 Hz frequency. This range varies from 0 t0 140 V/m for the same waveform using 1 MHz current pulse.

When the sinusoidal current pulse is applied, the recorded electric field range is 0 to 25 V/m for 10 Hz and 0 to 45 V/m for 1 MHz current pulses. Thus, the simulation frequency is proportional to the induced electric field over the RIO. It is interestingly shown that the direction of the lower simulation frequency is from the outer to towards to the centre. However, this is from the centre to towards the outer for the higher frequency level. This is valid for both simulation waveforms. It is noted that the electric field distribution is smoother for the higher simulation frequency compared to the lower frequency level.

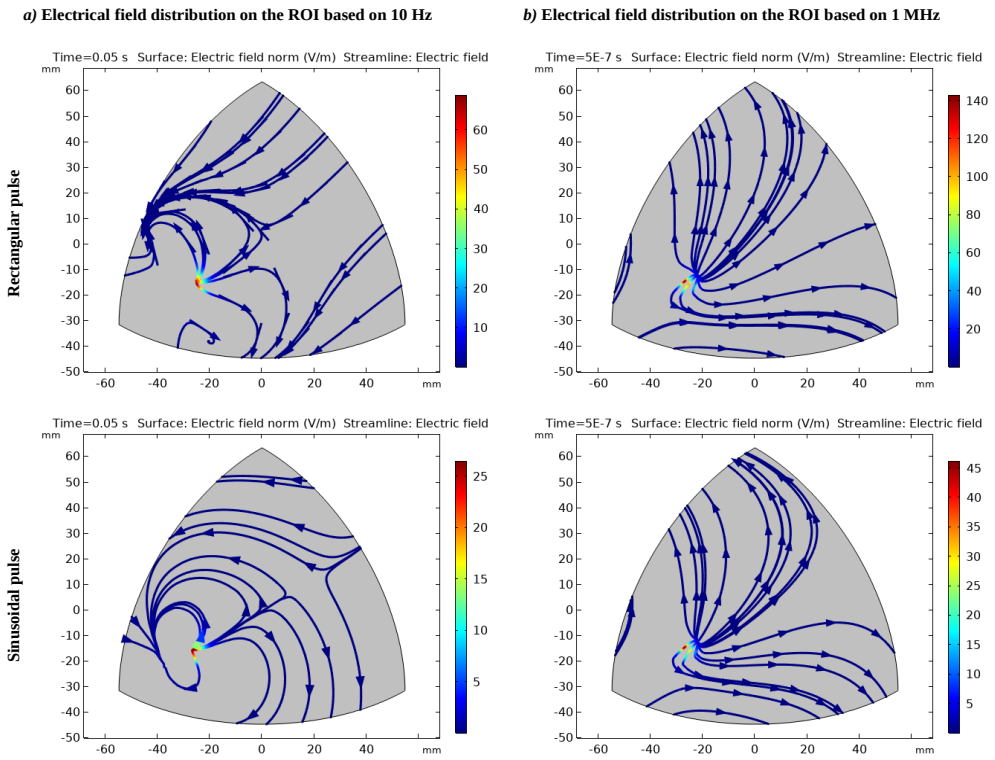

Figure 7. (***a***) Shows electric field distribution over the RIO for rectangular and sinusoidal waveforms based on 10 Hz. (***b***) Shows electric field distribution over the RIO for rectangular and sinusoidal waveforms based on 1 MHz.

4. Discussion

It has been shown that there are various factors influencing the DBS performance including waveform shape, frequency, pulse width [17]. It may not be feasible to deeply investigate the impact of such parameters on the outcome using experimental tests. Bio-modelling is increasingly becoming an alternative option to the design and optimization of biomedical devices. Thus, the impact of the simulation waveform shape and frequency level on the current density, electrical potential and electrical field variations was evaluated using such bio-computational modelling methods. A multi-layered bio-computational model of the human head was developed based on the previous study [3]. The electrode model was generated based on commercially available device parameters to analyse the impact of device stimulation waveforms using different frequencies. Also, the framework of the existing simulation software was highlighted for bio-computational model designers. The important steps of the generation of the volume conductor were emphasized. The results were calculated based on the time-dependent study by including the capacitive effect of the tissue layers.

The results showed that the amplitude of the electrical potential variation was reduced when the higher simulation frequency was applied as shown in Fig. 5. This can be associated with the composition of the body. When the higher frequency was used, the current penetrates to the inner structures as the simulation current pulse based on the higher frequency penetrates easily through the inner structures [15], and this led to lower induced electrical potential variation according to (2). Also, it was shown that the capacitive effect was more dominant when the higher frequency level was used based on rectangular waveform shape. This may be related to the sharp transition region of the rectangular pulse compared to the sinusoidal pulse.

It is shown that the induced electrical potential variation on the simulation electrodes distorted when the rectangular simulation waveform was used. This may be associated with sharpness of the transition region. Since the sinusoidal waveform has a smooth transition from anode to cathode region, whereas, rectangular has a significant sharp transition when the polarity was changed from anode to cathode (or vice-versa), thus, the results for rectangular waveform were more distorted based on higher frequency ranges.

Although the induced current density range is nearly the same for the different frequency levels and simulation waveform shapes, it was indicated in Fig. 6 that current density has more spread contours using a higher frequency. It is well known that the neuromodulator device based on higher frequency stimulation may spread the inner structure of the biological tissue layers with ease. The reason for current density range is nearly the same for the different frequency levels may be related to the geometric features of the electrode and the applied current level. Since the same electrode and the same current amplitude were used for this study; it is expected to be the same amount of the current density at the RIO for different simulation waveforms and frequency levels.

In Fig. 7, it was shown that the electric field variation was proportional to the simulation frequency for both simulation waveform types. This may be associated with the composition of the body as the simulation frequency increased and the induced electric field also increased.

Although some previous studies did not include the capacitive effect when the DBS based on FEM was studied [21, 22], the other was considered to compute the potential and current distribution that was resulting from the DBS [23]. The result of this study is in agreement with the existing study [23] regarding the capacitive effect. It has been shown that the capacitive affect has a substantial impact on the outcome. However, only this study investigates the impact of the different pulse waveforms based on different frequency levels using FEM procedures.

Overall, it can be deduced from the results of this study that the simulation waveform shape and simulation frequency level affect the performance of the DBS neuromodulator. The capacitive effect should not be ignored at the higher frequency levels, and it was also suggested that current density evenly distributed over the RIO at the higher frequency levels. These steps should be considered when a DBS neuromodulator is designed.

5. Conclusion

The multilayered bio-computational model was used to analyse the electrical potential, current density, and electric field variations within the human head model via DBS electrodes that are commonly used in clinical research studies. The goal of this study was to investigate the impact of the stimulation waveform shape and simulation frequency level on the outcome using the DBS system. The results for the sinusoidal and rectangular charge-balanced stimulation waveforms were recorded based on different frequency ranges. Also, the general flow of the computational model development was highlighted. The results showed that the stimulation waveforms have a significant impact on the electrical and current density distributions on the RIO.

6. Author Contribution Statement

In the study, Author 1 contributed to forming the idea, making the design and finalising the wok.

7. Ethics committee approval and conflict of interest statement

There is no conflict of interest with any person / institution in the article prepared.

8. References

[1] N. A. Pelot, B. J. Thio, and W. M. Grill, "Modeling current sources for neural stimulation in COMSOL," Front. Comput. Neurosci., vol. 12, no. June, pp. 1–14, 2018.
[2] L.-J. Ren, Y. Yu, Y.-H. Zhang, X.-D. Liu, Z.-J. Sun, W.-J. Yao, T.-Y. Zhang, C. Wang, C.-L. Li, "Three-dimensional finite element analysis on cochlear implantation electrode insertion," Biomech. Model. Mechanobiol., Apr. 2022.
[3] E. Salkim, A. Shiraz, and A. Demosthenous, "Impact of neuroanatomical variations and electrode orientation on stimulus current in a device for migraine: A computational study," J. Neural Eng., vol. 17, no. 1, 2020.
[4] E. Salkim, A. Shiraz, and A. Demosthenous, "Influence of cellular structures of skin on fiber activation thresholds and computation cost," Biomed. Phys. Eng. Express, vol. 5, no. 1, p. 015015, 2018.
[5] A. Fellner, A. Heshmat, P. Werginz, and F. Rattay, "A finite element method framework to model extracellular neural stimulation," J. Neural Eng., vol. 19, no. 2, Apr. 2022.
[6] J. Martinek, Y. Stickler, M. Reichel, W. Mayr, and F. Rattay, "A novel approach to simulate Hodgkin-Huxley-like excitation with COMSOL Multiphysics," Artif. Organs, vol. 32, no. 8, pp. 614–619, 2008.
[7] F.-J. Pettersen, and J. O. Høgetveit, "From 3D tissue data to impedance using Simpleware ScanFE+IP and COMSOL Multiphysics – a tutorial," J. Electr. Bioimp., vol. 2, pp. 13–32, 2011.
[8] P. Marianelli, M. Capogrosso, L. B. Luciani, A. Panarese, and S. Micera, "A computational framework for electrical stimulation of vestibular nerve," IEEE Trans. Neural Syst. Rehabil. Eng., vol. 4320, no. c, pp. 1–13, 2015.
[9] L.-J. Ren, Y. Yu, Y.-H. Zhang, X.-D. Liu, Z.-J. Sun, W.-J. Yao, T.-Y. Zhang, C. Wang, C.-L. Li, "Three-dimensional finite element analysis on cochlear implantation electrode insertion," Biomech. Model. Mechanobiol., Apr. 2022.
[10] E. Salkim, M. Zamani, D. Jiang, S. R. Saeed, and A. Demosthenous, "Insertion guidance based on impedance measurements of a cochlear electrode array," Front. Comput. Neurosci., vol. 16, Jun. 2022.
[11] E. Salkim, A. N. Shiraz, and A. Demosthenous, "Computational study on transcutaneous frontal nerve stimulation: Simplification of human head model," in Proc. COMSOL Conf., Rotterdam, pp. 1–4, 2017.
[12] M. Zelechowski, G. Valle, and S. Raspopovic, "A computational model to design neural interfaces for lower-limb sensory neuroprostheses," J. Neuroeng. Rehabil., vol. 17, no. 1, pp. 1–13, 2020.
[13] Y. Ge et al., "Mediating different-diameter Aβ nerve fibers using a biomimetic 3D TENS computational model," J. Neurosci. Methods, vol. 346, Dec. 2020.
[14] S. Raspopovic, S. Capogrosso, and M. Micera, "A computational model for the stimulation of rat sciatic nerve using a transverse intrafascicular multichannel electrode," IEEE Trans. Neural Syst. Rehabil. Eng., vol. 19, no. 4, pp. 333–344, 2011.
[15] S. F. Cogan, "Neural stimulation and recording electrodes," Annu. Rev. Biomed. Eng., vol. 10, no. 1, pp. 275–309, 2008.
[16] K. M. Prakash, "An overview of surgical therapy for movement disorders," Neurology.
[17] N. Yousif, R. Bayford, and X. Liu, "The influence of reactivity of the electrode-brain interface on the crossing electric current in therapeutic deep brain stimulation," Neuroscience, vol. 156, no. 3, pp. 597–606, Oct. 2008.
[18] E. Salkim, "Analysis of tissue electrical properties on bio-impedance variation of upper limps," Turk. J. Electr. Eng. Comput. Sci., vol. 30, no. 5, pp. 1839–1850, 2022.
[19] E. Salkim, and Y. Wu, "Modeling of transcutaneous recording for bio-impedance analysis on the upper-arm," IEEE Access, vol. 11, pp. 107184–107193, 2023.
[20] C. R. Butson, and C. C. McIntyre, "Tissue and electrode capacitance reduce neural activation volumes during deep brain stimulation," Clin. Neurophysiol., vol. 116, no. 10, pp. 2490–2500, Oct. 2005.
[21] J. D. Johansson, and P. Zsigmond, "Comparison between patient-specific deep brain stimulation simulations and commercial system SureTune3," Biomed. Phys. Eng. Express, vol. 7, no. 5, Sep. 2021.

[22] A. M. Frankemolle-Gilbert, B. Howell, K. L. Bower, P. H. Veltink, T. Heida, and C. C. McIntyre, "Comparison of methodologies for modeling directional deep brain stimulation electrodes," PLoS One, vol. 16, no. 12, Dec. 2021.

[23] K. Butenko, C. Bahls, M. Schröder, R. Köhling, and U. Van Rienen, "OSS-DBS: Open-source simulation platform for deep brain stimulation with a comprehensive automated modeling," PLoS Comput. Biol., vol. 16, no. 7, Jul. 2020.